Enhanced lasing assisted by the Ag-encapsulated Au plasmonic nanorods

Shuya Ning, Zhaoxin Wu,* Hua Dong, Fang Yuan, Jun Xi, Lin Ma, Bo Jiao, and Xun Hou

Key Laboratory of Photonics Technology for Information, Department of Electronic Science and Technology, School of Electronic and Information Engineering, Xi'an Jiaotong University, Xi'an 710049, China

**Corresponding author: zhaoxinwu@mail.xjtu.edu.cn*

Received October 24, 2014; revised January 22, 2015; accepted January 27, 2015; posted February 2, 2015 (Doc. ID 225664); published March 10, 2015

Threshold reduction and emission enhancement were reported for the waveguided random lasing, assisted by the Ag-encapsulated Au nanorods (Au@Ag NRs). The blend of tris(8-hydroxyquinolinato)aluminum (Alq_3) and 4-(dicyanomethylene)-2-tert-butyl-6(1,1,7,7-tetramethyljulolidyl-9-enyl)-4 H-pyran (DCJTB), which comprise the typical donor–acceptor lasing system, is used as the gain media. Compared with the Ag nanoparticles and Au nanorods, Au@Ag NRs exhibited the broad absorption spectra of localized surface plasmon resonance (LSPR) with multiple peaks, which sufficiently overlapped with both absorption and emission spectra of the donor–acceptor system of the gain media. This unique plasmonic characteristic of Au@Ag NRs leads to the lower lasing threshold and enhances the lasing efficiency by the effects of both enhancement of localized electromagnetic field and scattering.

OCIS codes: (140.3460) Lasers; (290.4210) Multiple scattering; (290.5850) Scattering, particles.
http://dx.doi.org/10.1364/OL.40.000990

Random lasing, based on the localized surface plasmon resonance (LSPR) [1,2] of metallic nanoparticles (NPs), has attracted significant attention for its interesting physical mechanism and potential value in applications [1–5]. In previous reports, the lasing threshold was reduced and its emission was greatly enhanced by the introduction of silver or gold NPs [6–12]. It is generally recognized that metal NPs enhance the lasing efficiency via two different mechanisms [6]: the enhancement of a localized electromagnetic (EM) field in the vicinity of metal NP, and the improvement of scattering effect, resulting from the large scattering cross section of metal NP. As for the applications of gold NPs, Popov *et al.* utilized gold NPs to enhance the lasing from a polymer film doped with Rhodamine 6G (Rh6G) [6,7]. Zhai and Zhang demonstrated an enhanced waveguided random laser of dye-doped polymer on gold nano-island structures [8]. Heydari *et al.* reported the emission enhancement in the plasmon assisted random laser by coupling between the dyes and the LSPR of Au NPs [9]. In these works, there was sufficient overlap between the LSPR spectra of Au NPs and emission spectra of the dyes; the scattering effect on the emitted light of gain media was considered to be the dominant mechanism to enhance lasing properties. As for the case of Ag NPs, Dice *et al.* demonstrated incoherent random lasing from a suspension of Ag NPs in a methanol solution of Rh6G [10]. Then, Meng *et al.* achieved the enhanced emission of coherent random lasing in polymer films by introducing Ag NPs [11,12]. In those works, because of the overlap between the LSPR spectra of Ag NPs and the absorption of dyes, the enhanced localized EM field was considered to be the dominant mechanism for the occurrence of random lasing, especially for the sizes of Ag NPs below 50 nm. It is anticipated that the random lasing could be induced by the effects of both scattering and an enhanced localized EM field of metallic nanostructure, which requires the LSPR spectra of the metallic nanoparticles to cover both the absorptions and emissions of lasing dyes.

However, the lasing dyes generally have the large stoke shifts between their absorptions and emissions, which could reduce the self-absorption and achieve the lower lasing threshold, especially for the donor–acceptor system, such as the blend of tris(8-hydroxyquinolinato)aluminum (Alq_3) and 4(dicyanomethy-lene)-2-tert-butyl-6 (1,1,7,7-tetramethyljulolidyl-9-enyl)4 H-pyran (DCJTB) [13,14]. However, the LSPR spectra of Ag or Au NPs are too narrow to overlap the spectra of both absorption and emission of lasing dyes [6–12]. Therefore, it hardly takes full advantage of both enhanced localized EM field and scattering effect to enhance lasing behavior.

In this Letter, the Ag-encapsulated Au nanorods (Au@Ag NRs) were explored and introduced into the gain media of the blend of Alq_3 and DCJTB. This plasmonic composite showed the broad spectrum of LSPR with multiple peaks, which covered both the absorption and emission spectra of the blend of Alq_3 and DCJTB. Compared with the gain media with Ag NPs or Au nanorods (Au NRs), the lowest lasing threshold of the gain media with Au@Ag NRs was achieved because of the unique plasmonic property of Au@Ag NRs.

The uncoated Au NRs were prepared by a seed-mediated growth method in aqueous solutions and were stabilized with cetyltrimethylammonium bromide (CTAB). Then, the Au@Ag NRs were prepared [15]. 2 mL of the uncoated Au NRs solution were centrifuged and redispersed into an aqueous cetyltrimethylammonium chloride (CTAC) solution at the same volume. 0.4 mL 0.01M aqueous $AgNO_3$ and 0.2 mL ascorbic acid solutions were then added to produce Ag coating. Figure 1 shows the transmission electron microscopy (TEM) and scanning electron microscopy (SEM) images of Au@Ag NRs. The shapes and sizes of the nanorods are relatively uniform. The average length and diameter of Au core are 65 ± 4 nm and 15 ± 2 nm. The average thicknesses of the Ag shell are 8.0 and 2.0 nm at the side and ends, respectively.

The Au@Ag NR aqueous solution was then spin-coated onto glass substrate at 450 rpm and dried at 80°C, and the Au@Ag NRs island film was obtained. Finally, the

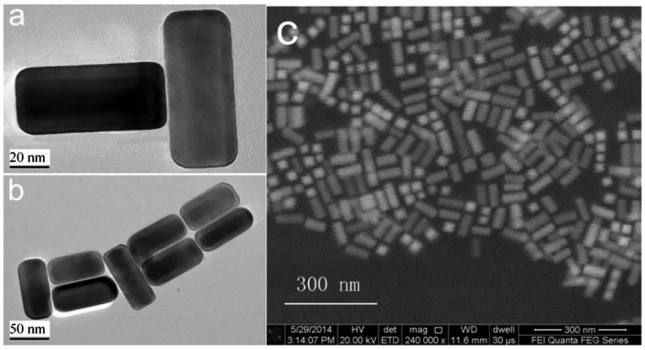

Fig. 1. (a) and (b) TEM images of the Au@Ag NRs, and (c) SEM image of the Au@Ag NRs.

planar waveguide with gain media was fabricated as follows: Polystyrene (PS), Alq_3, and DCJTB were fully dissolved in a chloroform solution (PS: Alq_3: DCJTB = 200:100:3.5, wt. %), and then spin-coated onto Au@Ag NRs island film at the speed of 3000 rpm. For comparison, the device with Ag NPs (diameter ~50 nm) and that with Au NRs (average length and diameter are 65 ± 4 nm and 15 ± 2 nm) were prepared as in the above procedure. The film thickness is approximately 250 nm and the structure of the device is shown as Fig. 2(a). The samples were pumped by the third harmonic of Nd: YAG laser (355 nm, 10 Hz repetition rate, and 25 ps pulse duration). Through a pinhole filter, a slit, and a cylindrical lens, the laser beam was formed as a stripe with the size of 7 mm × 1 mm, and was perpendicular to the surface of the devices.

The absorption spectra, that is, the LSPR spectra of Au@Ag NRs, Ag NPs, and Au NRs were shown as Fig. 2(b). The "rod-like" metallic nanostructures generally have the longitudinal and transverse plasmon resonances which correspond to two peaks. In our experiments, the LSPR peak of Ag NPs is 437 nm, and that of Au NRs before Ag coating are 828 and 521 nm. As for the Au@Ag NRs, there are four LSPR peaks (343, 390, 437, and 640 nm). The peaks of 640 and 437 nm (390 and 343 nm) are ascribed to the longitudinal and transverse dipolar plasmon mode of Au (Ag). The blue shift of longitudinal and transverse surface plasmon wavelength of Au can be attributed to the coating of the Ag shell [15]. In Fig. 2(b), the absorption and emission spectra of Alq_3 and DCJTB are shown. Alq_3: DCJTB is the gain media which is a typical donor–acceptor reported in previous reports. Alq_3 is used as a donor and DCJTB is used as an acceptor, which are the Förster resonance energy transfer system [16]. It could be clearly seen that the donor emission, centered around 518 nm, overlaps well with the acceptor peak at 512 nm, enabling efficient resonant energy transfer between the donor and acceptor. According to Fig. 2(b), compared with the Ag NPs and Au NRs, the LSPR with multiple peaks of Au@Ag NRs has a considerable overlap with both the absorption of Alq_3 and emission spectra of DCJTB.

Too demonstrate the emission properties of the device with Au@Ag NRs, the devices without metallic NPs were prepared. Figure 3(a) shows the edge-emission spectra of the gain medium without metallic NPs. As described in previous reports [17], the neat gain medium film exhibits an obvious lasing behavior. When it is pumped at low

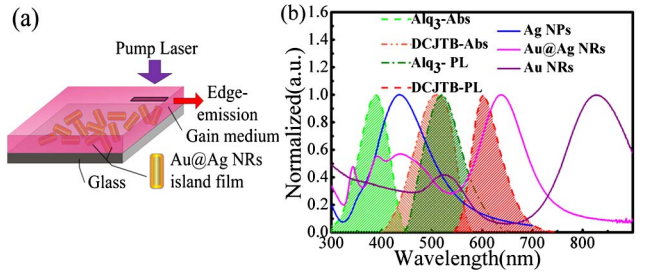

Fig. 2. (a) Structure of gain medium Au@Ag NRs. (b) The LSPR spectra of Au@Ag NRs, Ag NPs, and Au NRs with the absorption and emission of Alq_3 and DCJTB.

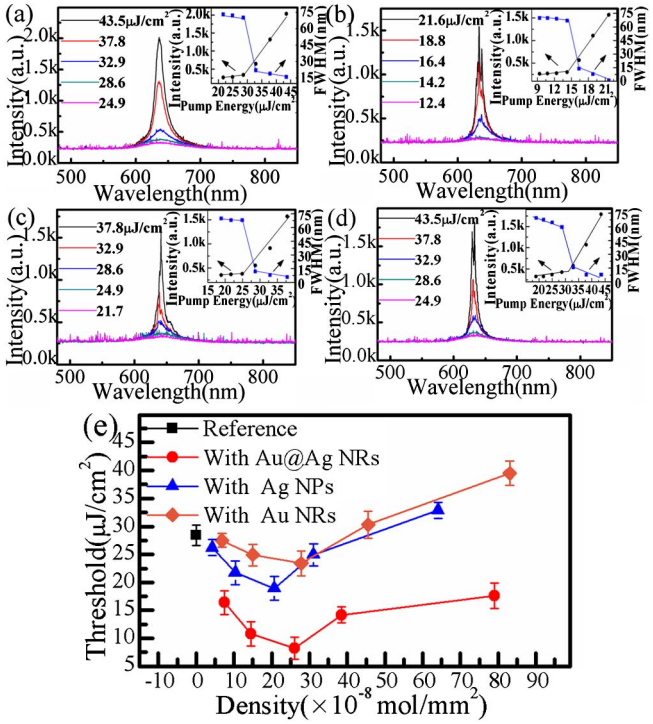

Fig. 3. Emission spectra of the device (a) without nano structures, (b) with the Au@Ag NRs; the density is 3.85×10^{-7} mol/mm^2, (c) with the Ag NPs; the density is 3.11×10^{-7} mol/mm^2, and (d) with the Au NRs; the density is 4.55×10^{-7} mol/mm^2. The corresponding insets show the lasing intensity and the FWHM of the emission spectra on the pump energy intensity. (e) Dependence of lasing threshold on density of Au@Ag NRs (red circle), Ag NPs (blue triangle), and Au NRs (orange diamond).

energy, it exhibits a broad spontaneous emission spectrum with full width at half-maximum (FWHM) of 75 nm. Once the excitation energy becomes large enough, the emission spectrum collapses to a much narrower emission with FWHM of 15 nm. The lasing threshold of 28.6 μJ/cm^2 is determined [see Fig. 3(a)].

As shown in previous reports [10], the lasing threshold of gain media with silver NPs depends on the density of silver NPs. In our experiment, to achieve the optimized condition of lasing, the different densities of Au@Ag NRs island films was prepared. In addition, the densities ranged from 7.5×10^{-8} to 7.9×10^{-7} mol/mm^2, with atomic force microscopy (AFM) images shown in Fig. 4.

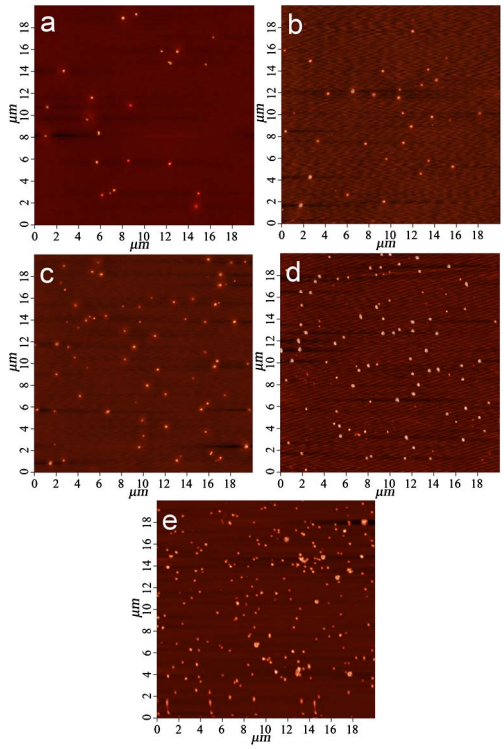

Fig. 4. AFM images of different densities of Au@Ag NRs island films. The density is (a) 7.5×10^{-8} mol/mm^2, (b) 1.45×10^{-7} mol/mm^2, (c) 2.6×10^{-7} mol/mm^2, (d) 3.85×10^{-7} mol/mm^2, and (e) 7.9×10^{-7} mol/mm^2, respectively.

Figure 3(b) shows the edge-emission spectra of the device with Au@Ag NRs, in which the density is 3.85×10^{-7} mol/mm^2. It presents the characteristics of coherent random lasing because of the emergence of the sharp spikes in emission spectra. When the excitation energy reaches the threshold, the spectrum suddenly becomes narrow, and the FWHM reduces to about 1 nm. For comparison, the device based on Ag NPs and Au NRs island films was also prepared; the densities were varied from 4.2×10^{-8} to 6.4×10^{-7} mol/mm^2 for Ag NPs and 6.8×10^{-8} to 8.3×10^{-7} mol/mm^2 for Au NRs, respectively. The emission spectra of the device with Ag NPs or Au NRs are shown in Figs. 3(c) and 3(d), which also exhibit coherent random lasing. Figure 3(e) illustrates the variation of lasing thresholds for the gain media with different densities of Au@Ag NRs, Ag NPs, and Au NRs island film. It shows that, with the increasing of their density, the lasing threshold reduces at first, and then increases. The lowest lasing threshold of gain medium with Au@Ag NRs is 8.2 μJ/cm^2 for the density of 2.6×10^{-7} mol/mm^2, with Ag NPs being 18.9 μJ/cm^2 for the density of 2.07×10^{-7} mol/mm^2, and that with Au NRs is 23.4 μJ/cm^2 for the density of 2.78×10^{-7} mol/mm^2. Compared with the device with Ag NPs or Au NRs, the device with Au@Ag NRs has the lowest lasing threshold, and lasing property has been greatly enhanced, as shown in Table 1.

To fully demonstrate the enhancement characteristics of the device with Au@Ag NRs, the net gains of media on Au@Ag NRs island films were studied in detail. The net gain was measured by the variable-stripe-length method which observes laser emission from the film edge as a function of excitation length. The output emission $I(\lambda)$ should obey the following equation [18]:

$$I(\lambda) = \frac{A(\lambda) I_P}{g(\lambda)} (e^{g(\lambda)L} - 1), \tag{1}$$

where $A(\lambda)$ is a constant related to the cross section for spontaneous emission, I_p is the pump intensity, g is the net gain coefficient, and L is the length of the pumped stripe. Figure 5(a) shows the spectra intensities of devices with the density of Au@Ag NRs from 7.5×10^{-8} to 7.9×10^{-7} mol/mm^2, each as a function of excitation length at 37.8 μJ/cm^2 pump influence. The experimental data and the solid curves in Fig. 5(a) are then fitted with Eq. (1), giving net gains of 23.5, 31.4, 36.2, 25.5, and 20.6 cm^{-1} for the devices with increasing density of Au@Ag NRs, and 16.8 cm^{-1} for the device without metallic NPs. Figure 5(b) shows that with the increasing of Au@Ag NR density, the gain increases at first, and then reduces. The maximum of net gain is achieved when the density is 2.6×10^{-7} mol/mm^2, which leads to the lowest lasing threshold of organic gain media.

As we know, the metallic NPs have been used to enhance the lasing efficiency [6–12], and the two different mechanisms are accepted as: (a) enhancement of localized EM field in the vicinity of metal NPs and (b) enhancement of scattering strength [6]. The effect of the enhanced localized EM field can increase the density of pump light available for the gain media, and consequently increases the probability that more dye molecules are excited simultaneously to the higher energy levels; then the excitation (pump) rate can be enhanced. This is guaranteed by the overlap between the LSPR spectra and the absorption of the Alq_3. On the other hand, it is also able to increase the quantum yield of the gain media depending on the degree of the overlap between the LSPR spectra and the emission of the DCJTB. As for the effect of scattering, when metallic NPs are excited resonantly, they scatter the energy of

Table 1. Threshold of Devices with Au@Ag NRs ($E_{\text{th-Au@Ag}}$), Ag NPs ($E_{\text{th-Ag}}$), Au NRs ($E_{\text{th-Au}}$) for Different Densities of Au@Ag NRs ($\rho_{\text{Au@Ag}}$), Ag NPs (ρ_{Ag}) and Au NRs (ρ_{Au})

$\rho_{\text{Au@Ag}}$ ($\times 10^{-8}$ mol/mm^2)	$E_{\text{th-Au@Ag}}$ (μJ/cm^2)	ρ_{Ag} ($\times 10^{-8}$ mol/mm^2)	$E_{\text{th-Ag}}$ (μJ/cm^2)	ρ_{Au} ($\times 10^{-8}$ mol/mm^2)	$E_{\text{th-Au}}$ (μJ/cm^2)
7.5	16.4	4.2	26.2	6.8	27.5
14.5	10.8	10.3	21.7	15	24.9
26	8.2	20.7	18.9	27.8	23.4
38.5	14.2	31.1	24.9	45.5	30.3
79	17.6	64	32.9	83	39.5

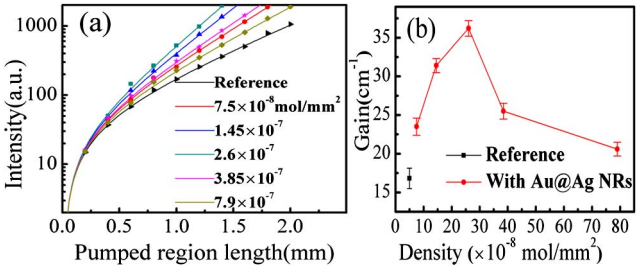

Fig. 5. (a) Dependences of emission intensity on the excitation length at 37.8 μJ/cm^2 pump intensity for devices with different densities of Au@Ag NRs island film. (b) The gains as a function of different densities of Au@Ag NRs.

emitters with the greater scattering cross sections, and then easily lead to the occurrence of random lasing. Therefore, comparing with the absorption spectra of the Ag NPs and Au NRs, the multi-LSPR peaks and broader absorption spectra of Au@Ag NRs have a sufficient overlap with both the absorption of Alq_3 and the emission of DCJTB so that the two mechanisms mentioned above all function well, which is expected to be the reason for the lowest lasing threshold.

In addition to the broad spectra and multi-peak of LSPR of Au@Ag NR, the unique "plasmonic hot spot" characteristic, which results from the sharp edges and corners of the metal nanostructures, could focalize the EM field at the corners or the edges. Then, very large enhancement factors of the electric field can be obtained. To further confirm the enhanced local field of the Au@Ag NRs, three-dimensional models of three nanostructures were built. The finite difference time-domain method (FDTD) was applied to calculate the electric-field distribution near to the Au@Ag NRs, Ag NPs, and Au NRs. Figure 6 shows the FDTD simulation of the electric-field distribution of the Au@Ag NRs, Ag NPs, and Au NRs with different exciting wavelengths at 355 and 630 nm which are wavelengths of pump light and emission light, respectively. The color scale indicates the electric field enhancement factors, normalized to the incident wave. It is found that the electrical field of the Au@Ag NRs obviously enhanced compared with that of the Ag NPs and Au NRs. At the same time, we find that the electrical field of the Ag NPs is stronger than that of Au NRs. This is because the Ag nanocrystals exhibit much stronger electric field enhancements than those of Au nanocrystals [15]. The simulation confirmed the unique local field enhancement of the Au@Ag NRs, which plays the important role in plasmonic enhanced lasing.

In conclusion, a unique Au@Ag NR was prepared and applied to the gain media of the donor–acceptor system. We found that the plasmonic Au@Ag NRs significantly improved the lasing efficiency of the organic gain medium and achieved the lower lasing threshold than that of the device with Ag NPs and Au NRs. The broader absorption and multi-peaks of LSPR of Au@Ag NRs overlapped sufficiently with both the absorption and emission spectra of the donor–acceptor of the gain medium, which resulted in the enhanced lasing by the effects of both enhanced localized EM field and scattering. Our work provides an ideal way to achieve low-threshold for plasmon-based random lasing by tuning the LSPR spectra of metallic nanostructures.

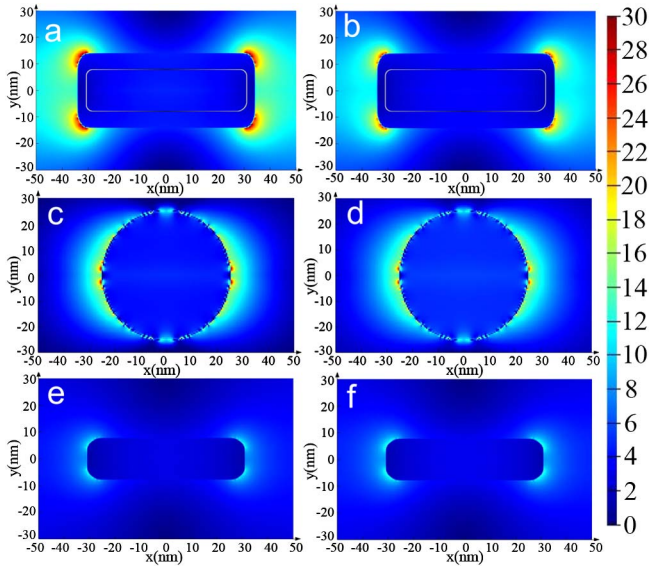

Fig. 6. Distribution of electric field normalized to the incident wave at the wavelengths of (a), (c), (e) 355 nm, (b), (d), (f) 630 nm near the Au@Ag NRs, Ag NPs, and Au NRs.

This work was financially supported by the Basic Research Program of China (2013CB328705), the National Natural Science Foundation of China (Grant Nos. 61275034 and 61106123), Ph.D. Programs Foundation of Ministry of Education of China (Grant No. 20130201110065), and Fundamental Research Funds for the Central Universities (Grant No. xjj2012087).

References

1. K. Aslan, I. Gryczynski, J. Malicka, and E. Matveeva, Curr. Opin. Biotechnol. **16**, 55 (2005).
2. J. R. Lakowicz, Anal. Biochem. **337**, 171 (2005).
3. M. I. Stockman, Nat. Photonics **2**, 327 (2008).
4. H. A. Atwater, Nat. Mater. **9**, 205 (2010).
5. H. Cao, Phys. Rev. Lett. **82**, 2278 (1999).
6. O. Popov, A. Zilbershtein, and D. Davidov, Polym. Adv. Technol. **18**, 751 (2007).
7. O. Popov, A. Zilbershtein, and D. Davidov, Appl. Phys. Lett. **89**, 191116 (2006).
8. T. Zhai and X. Zhang, Nano Lett. **11**, 4295 (2011).
9. E. Heydari, R. Flehr, and J. Stumpe, Appl. Phys. Lett. **102**, 133110 (2013).
10. G. D. Dice, S. Mujumdar, and A. Y. Elezzab, Appl. Phys. Lett. **86**, 131105 (2005).
11. X. Meng, K. Fujita, Y. Zong, and S. Murai, Appl. Phys. Lett. **92**, 201112 (2008).
12. X. Meng, K. Fujita, S. Murai, and K. Tanaka, Phys. Chem. A **79**, 053817 (2009).
13. S. Ning, X. Zhao, H. Dong, F. Yuan, L. Ma, B. Jiao, and X. Hou, Org. Electron. **15**, 2052 (2014).
14. W. Lu, H. You, and D. Ma, Appl. Opt. **46**, 2320 (2007).
15. R. Jiang and H. Chen, Adv. Mater. **24**, OP200 (2012).
16. M. Lehnhardt, T. Riedl, T. Weimann, and W. Kowalsky, Phys. Rev. B **81**, 1652061 (2010).
17. F. Hide and B. J. Schwartz, Science **273**, 1833 (1996).
18. M. D. McGehee, R. Gupta, S. Veenstra, and E. K. Miller, Phys. Rev. B **58**, 7035 (1998).